Evidence for isotopically light Fe mobility under oxidising conditions in subduction zone fluids: A record of Monviso meta-serpentinites, Western Alps

Baptiste Debret, Clara Caurant, Bénédicte Ménez, Vincent Busigny, Frédéric Moynier

Earth Planet. Sci. Lett. 642 (2024) 118855

Contents lists available at ScienceDirect

Earth and Planetary Science Letters

journal homepage: www.elsevier.com/locate/epsl

Evidence for isotopically light Fe mobility under oxidising conditions in subduction zone fluids: A record of Monviso meta-serpentinites, Western Alps

Baptiste Debret *, Clara Caurant, Bénédicte Ménez, Vincent Busigny, Frédéric Moynier

Université Paris Cité, Institut de physique du globe de Paris, CNRS, Paris, France

ARTICLE INFO

Keywords:
Subduction
Fe isotopes
Serpentinites

ABSTRACT

The isotopically light Fe signature of arc magmas relative to mid-oceanic ridge basalts (MORB) is expected to be related to the redox state of their source. This implies a link between Fe mobility and redox variations across subduction zones. Here we address slab chemical variations during prograde metamorphism through a comprehensive geochemical study, including major, trace elements and Fe stable isotope (δ^{56}Fe) analyses, of meta-serpentinites composing the eclogitic meta-ophiolite of the Monviso massif (Western Alps, Italy). These rocks partly preserve mantle related geochemical heterogeneities, as supported by negative correlations between fluid immobile elements (High Field Strong Elements) and LREE/HREE (Light – Heavy Rare Earth Elements) ratios. They are however characterized by large Cs enrichments relative to U or alkali elements suggesting that abyssal fluid mobile elements signature was overprinted by subduction related processes. Meta-serpentinites display large δ^{56}Fe variations, from -0.20 ± 0.05 ‰ to +0.09 ± 0.03 ‰. Mineral separate analyses of olivine bearing veins show low Δ^{56}Fe between olivine and magnetite (~ 0.4 ‰), which according to Fe isotope thermometry correspond to high temperature equilibration, estimated between 530 and 550 °C, compatible with Monviso metamorphic climax (520–570 °C and 2.6–2.7 GPa). These results, in combination with geochemical modelling, confirm a reset of δ^{56}Fe signature of abyssal serpentinites during prograde metamorphism in subduction zones. The bulk rock δ^{56}Fe values of Monviso meta-serpentinites are negatively correlated with their $Fe^{3+}/\sum Fe$ and As concentrations (a redox-sensitive and fluid mobile element). These correlations can be attributed to a metasomatism by external fluids derived from slab serpentinites during subduction. It also concords with the oxygen fugacity (fO_2) record in meta-serpentinites, with meta-serpentinites equilibrated at high fO_2 displaying the lowest δ^{56}Fe values while samples equilibrated at low fO_2 display mantle like δ^{56}Fe signatures. These results highlight that oxidising conditions during serpentinite dehydration are likely to boost isotopically light Fe mobility in slab derived fluids.

1. Introduction

Subduction zone is a key geological setting for the global cycling of redox-sensitive elements such as oxygen (O), iron (Fe), sulfur (S), carbon (C), hydrogen (H) and nitrogen (N). However, the net fluxes of these elements through the subduction are poorly constrained (Evans, 2012). Furthermore, there are ongoing controversies surrounding the processes controlling redox-sensitive elements abundances and mobility during subduction. The understanding of redox-sensitive element transfers in subduction zones was initially approached by examining the composition of arc magmas. These magmas have high $Fe^{3+}/\sum Fe$ ratio and volatile contents compared to mid-oceanic ridges basalts (MORB; Arculus, 1994; Brounce et al., 2015; Gaborieau et al., 2020; Kelley and Cottrell, 2009). This suggests that the mantle wedge peridotites, which is the source for arc magmas, were metasomatized by slab derived fluids equilibrated at high oxygen fugacity (fO_2; e.g., CO_X, SO_X). However, the interpretation and significance of these results have been a subject of controversy. For example the study of V/*Sc* and Zn/Fe ratios in arc basalts have raised questioned on whether mantle wedge peridotites are more oxidized than the mantle source of the MORB (Lee et al., 2010, 2005). In order to gain further insights, the study of arc magma was then complemented by the analysis of the Fe redox state in residual slabs

* Corresponding author.
E-mail address: debret@ipgp.fr (B. Debret).

https://doi.org/10.1016/j.epsl.2024.118855
Received 26 May 2023; Received in revised form 13 June 2024; Accepted 15 June 2024
Available online 10 July 2024

exposed in mountain ranges, known as meta-ophiolites. Debret et al. (2014, 2015) were the first to report a gradual decrease of $Fe^{3+}/\sum Fe$ total and the dissolution of oceanic magnetite, coinciding with the progressive dehydration of serpentinites at high pressure (HP). These results were interpreted as indicative of an iron reduction during prograde metamorphism. This redox reaction could be coupled with the oxidation of reduced phases (e.g., sulfide, organic carbon), thereby facilitating the formation of highly oxidized fluids (e.g., SO_X; Debret and Sverjensky, 2017). However, the observed $Fe^{3+}/\sum Fe$ variations have been challenged by several studies, suggesting that these redox variations could be influenced by protolith composition and may not necessarily reflect changes in redox budget during subduction (Bretscher et al., 2018; Vieira Duarte et al., 2021).

Iron stable isotope composition ($\delta^{56}Fe$) provides key constraints for understanding the mobility and mass balance of redox-sensitive elements in subduction zones. During partial melting, ferric Fe is more incompatible than ferrous Fe leading to isotopically heavy Fe mobility in magmas (Dauphas et al., 2009; Sossi and Debret, 2021; Sossi and O'Neill, 2017). Surprisingly, arc magmas display lighter Fe isotopic signature than MORB. This can be reconciled through either multiple melt extraction events leaving a refractory sub-arc mantle residue with relatively light Fe isotopes and/or infiltration of isotopically light Fe-bearing fluids derived from the slab in their source (Chen et al., 2023; Dauphas et al., 2009; Foden et al., 2018; Nebel et al., 2015; Sossi et al., 2016). Theoretical models suggest that the mobility of Fe, and the resulting Fe isotopic fractionations, are driven by the presence of Cl^-, SO_4^{2-} and CO_3^{2-} anions, which preferentially complex with isotopically light iron (Fujii et al., 2014; Hill and Schauble, 2008). Given that these elements are ubiquitous and abundant in fluids derived from serpentinites (Scambelluri et al., 2015), Fe isotopes are potential tracers of these processes in subduction zones. In addition, the effects of seafloor alteration (i.e., role of protolith inheritance) on the $\delta^{56}Fe$ compositions of mantle peridotites are relatively limited (Craddock et al., 2013; Debret et al., 2016; 2018a), which makes easier the identification of subduction related fractionations. Hence, Fe isotopes were used to probe the speciation and redox state of slab-derived fluids in subduction zones. Several studies have reported significant $\delta^{56}Fe$ variations in subducted materials (Chen et al., 2019; Debret et al., 2021, 2016; Deng et al., 2022; El Korh et al., 2017; Gerrits et al., 2019; Inglis et al., 2017). In particular, Debret et al. (2016) employed Fe isotopes as a record of redox exchanges between fluid and rocks during serpentinite dehydration in subduction zones. These authors observed an increase of $\delta^{56}Fe$ value in serpentinites with increasing metamorphic grade in alpine meta-ophiolites. Based on a negative correlation with $Fe^{3+}/\sum Fe$, they interpreted these $\delta^{56}Fe$ variations as a response to extraction of isotopically light Fe as Fe-SOx or Fe-Cl from serpentinites during prograde metamorphism. However, this interpretation was recently questioned by Evans and Frost (2021) who speculated that the observed trends could also be attributed to variable composition of the rock protoliths from different geodynamic settings. Indeed, the entire range of Fe isotopic values measured by Debret et al. (2016) can be covered by variously serpentinized abyssal peridotites and rocks from different geodynamical settings, such as unmetamorphosed Purang ophiolite (Su et al., 2015), or unmetamorphosed abyssal serpentinites (Craddock et al., 2013).

Here we further investigate the role of HP metamorphism and redox processes on the variations in Fe stable isotope observed in HP meta-ophiolites by investigating the $\delta^{56}Fe$ signature of meta-serpentinites from the Monviso massif. The latter is a well-characterized section of oceanic lithosphere (Angiboust et al., 2012; Balestro et al., 2013, 2011; Locatelli et al., 2019a; Lombardo et al., 1978) that was subducted at eclogite facies P-T conditions (520–570 °C and 2.6–2.7 GPa) before being exhumed during alpine orogeny. This massif is an ideal target to test Fe mobility associated with redox variation during serpentinite dehydration in a subducting slab, hence avoiding comparison between different geological settings. Indeed, Caurant et al. (2023) proposed, based on thermodynamic models and petrological observations, that the meta-ophiolite recorded significant redox heterogeneities imposed during eclogite facies metamorphism, with oxygen fugacity (fO_2) ranging from +2 relative to Fayalite-Magnetite-Quartz (FMQ) buffer to FMQ −4. We show here that these redox variations are associated with large variations in $Fe^{3+}/\sum Fe$ and $\delta^{56}Fe$ values, with samples equilibrated at high fO_2 displaying the highest $Fe^{3+}/\sum Fe$ ratios and the lightest Fe isotopes values. Furthermore, mineral separate analyses of co-existing olivine and magnetite show a $\Delta^{56}Fe_{Mgt\text{-}Ol}$ value of approximatively 0.4 ‰, which is lower than that of abyssal serpentinites ($\Delta^{56}Fe_{Mgt\text{-}Ol} \sim 0.8$ ‰). This value is consistent with high temperature equilibrium, estimated from 530 to 550 °C using the olivine-magnetite thermometers proposed by Sossi and O'Neill (2017) and Rabin et al. (2021). These temperature estimates overlap with inferred peak P-T of Monviso massif. These results demonstrate a reset of $\delta^{56}Fe$ values at HP-HT during prograde metamorphism, and imply that the negative correlation between $Fe^{3+}/\sum Fe$ and $\delta^{56}Fe$ values in meta-serpentinites reflects Fe mobility at the massif scale during subduction-related metamorphic processes. This geochemical correlation confirms previous results by Debret et al. (2016) in Western Alps serpentinites. Interestingly, the most fractionated samples are equilibrated at high fO_2, while samples equilibrated at low fO_2 display mantle like values. Therefore, our results suggest that the dehydration of serpentinites under oxidising conditions is likely to enhanced the mobility of isotopically light Fe in metamorphic fluids.

2. Geological setting and sampling

Our study focuses on ultramafic rocks sampled along the Monviso meta-ophiolite (Fig. 1). The latter extends over 30 km at the French-Italian border and belongs to the Ligurian Piemontese domain in the Western Alps. It is separated from the blueschist-facies Queyras Schistes Lustrés Complex to the West and from the eclogite-facies Dora Maira continental unit to the East by two ductile normal faults (Ballèvre et al., 1990). Over the last decades, successive field, petrological and geochemical studies performed on the Monviso meta-ophiolite have refined interpretations of its tectonic structure, highlighting the existence of two coherent oceanic units, namely the Upper and Lower Tectonic Units, separated by west-dipping shear zones (Fig. 1; Angiboust et al., 2012; Locatelli et al., 2019; Lombardo et al., 1978). Those have recorded different pressure-temperature (P-T) conditions, of about 480 °C/2.2 GPa and 520–570 °C / 2.6–2.7 GPa, respectively (Angiboust et al., 2012; Caurant et al., 2023; Schwartz et al., 2001). They were then juxtaposed at epidote–blueschist facies during alpine orogeny and are now separated by an alpine related West-dipping shear zone, namely the Upper Shear Zone (Fig. 1; Angiboust et al., 2012). The studied rocks were sampled along the Lower Tectonic Unit. Despite a complex metamorphic history, this unit could partly derive from an oceanic core complex (Balestro et al., 2015; Caurant et al., 2023), preserving the original lithostratigraphy of a heterogeneous crustal section such as the ones observed at slow-spreading ridges or in other Western Alps (meta-) ophiolites (Lagabrielle and Cannat, 1990). In the Northern massif, the Lower Tectonic Unit includes from East to West a succession of deep-seated sequence, i.e., minor gabbroic intrusions into an extended section of serpentinized lithospheric mantle (basal serpentinites), to paleoseafloor sequence, i.e., metasediments sitting on paleoseafloor serpentinites. In the Southern massif, the Lower Tectonic Unit is characterized by scarce metasedimentary rocks and a large amount of metabasites. It consists, from East to West, of a thick sequence of metagabbros and meta-serpentinites sitting below metabasalts. To the East, the lower sheared zone (LSZ) separates metagabbros from the basal serpentinite unit. The LSZ includes highly deformed meta-ophidolomites and metabasites within a serpentinite matrix (thereafter named LSZ-serpentinites).

We selected 13 meta-serpentinites from the Northern part of the massif, including 3 basal (samples Vis20–1; Vis20–11; Vis20–14) and 10 seafloor (samples Vis18–4; Vis18–5A1; Vis18–5A2; Vis18–5B;

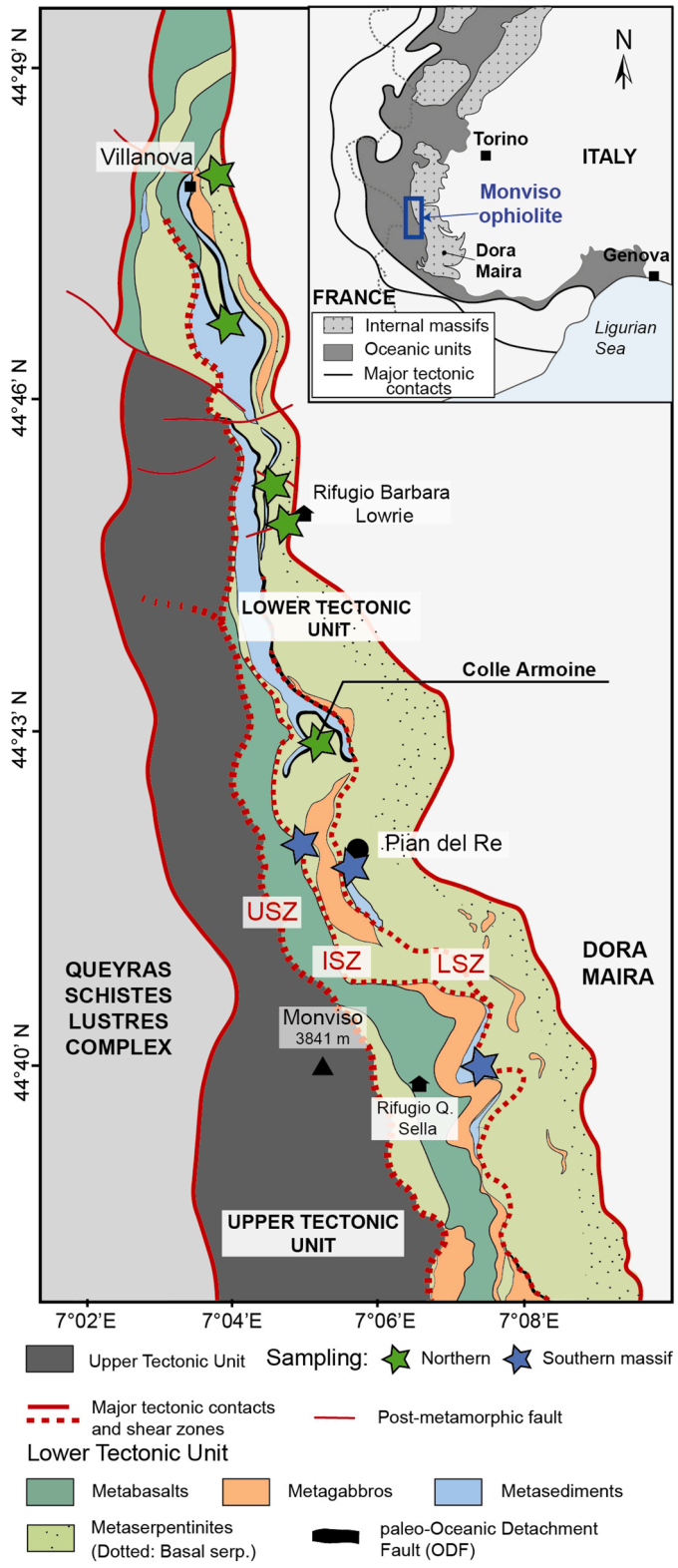

Fig. 1. Geological map of the Monviso meta-ophiolite showing the location of the studied samples.

Vis18–6A; Vis18–6B; Vis18–9; Vis20–5; Vis20–6; Vis20–10) serpentinites, and 3 LSZ-serpentinites from the Southern part of the massif (samples Vis18–1; Vis18–2; Vis18–3). The samples are mainly made of antigorite and metamorphic olivine locally associated with titano-humite, diopside, chlorite and/or brucite. These assemblages are formed at metamorphic climax through antigorite and brucite breakdown to metamorphic olivine, titano-humite and/or diopside (Caurant et al., 2023; Gilio et al., 2020; Schwartz et al., 2013). Despite a homogeneous P-T record, meta-serpentinite forming minerals are variable at massif scale. Such mineralogical variations were attributed to different fO_2 records, with basal serpentinites recording high fO_2 conditions (~ FMQ +2), while paleo-seafloor or LSZ-serpentinites record lower fO_2 conditions (~ FMQ −4), limiting magnetite crystallization (Caurant et al., 2023). The paleo-seafloor serpentinite can display residual calcite and are associated with abundant carbonaceous matter. In basal serpentinites, olivine is associated with abundant magnetite that often forms large veins of several centimetre width (Fig. 2). The preferential crystallization of metamorphic olivines in veins, relative to the host serpentinite, attests that they localized the fluid circulation and behaved as high permeability reaction zones during subduction. Exhaustive field and petrological description of the studied samples can be found in Caurant et al. (2023).

3. Methods

All samples were cut away from weathered surface, pen marks and sticker residues. They were then crushed with an agate mortar and a pestle, prior being powdered with an agate bowl. For the basal serpentinite sample VIS20–11, olivine veins (sample VIS20–11 V) were large enough to be milled separately from the host rock (sample VIS20–11CR). Additional magnetite crystals were micro-drilled in olivine vein (sample VIS20–11). All the bulk rock samples were then processed for major (SiO_2, Al_2O_3, $Fe_2O_3^T$, FeO, MnO, MgO, CaO, Na_2O, K_2O, TiO_2), volatile (C) and fluid mobile (B) elements at the Service of Analyses of Rocks and Minerals (SARM) in Nancy (France) and for trace (Li, Ti, V, Co, Ni, Cu, Zn, As, Rb, Sr, Y, Zr, Cd, Sb, Cs, Ba, La, Ce, Pr, Nd, Sm, Eu, Gd, Tb, Dy, Ho, Er, Tm, Yb, Lu, Ta, Pb, U) at the Institut de Physique du Globe de Paris (IPGP). Both bulk rock and microdrilled magnetites were processed for stable Fe isotopes at IPGP.

3.1. Major and volatile elements

Major elements analyses were carried out using a Thermo Scientific iCap6500 ICP-OES. Boron concentrations were measured by spectrophotometric determination. Samples were dissolved by fusion with anhydrous sodium carbonate following the procedures described by Carignan et al. (2001). Results for reference materials CRPG UB-N serpentinite analysed alongside the samples show a difference with literature values of less than 2 % for major elements (Appendix A). Volatile

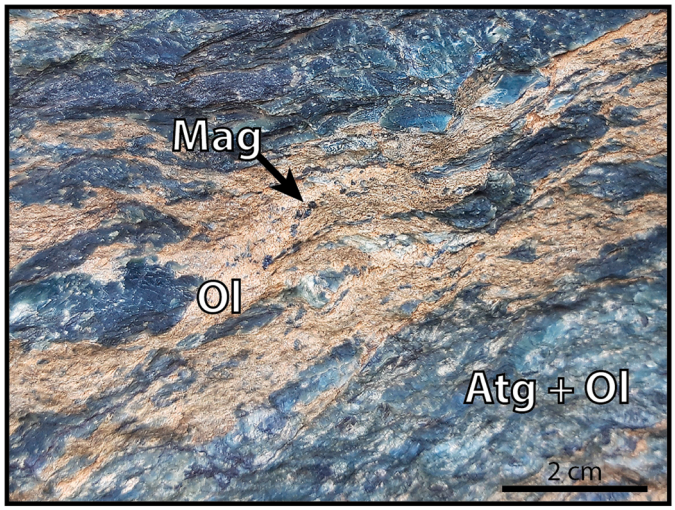

Fig. 2. Field photograph of meta-serpentinites outcropping in the Monviso meta-ophiolite. The meta-serpentinite is crosscut by olivine bearing veins associated with magnetite crystals of millimetre size.

(C) concentrations were analysed using a Leco CS230 Carbon/Sulphur Determinator. Additional FeO analyses were done by automatic titration at the equivalent point with potassium dichromate after dissolution of the sample in a HF/H_2SO_4 mixture, in the presence of H_3BO_3 and H_3PO_4. Subsequently, $Fe^{3+}/\Sigma Fe$ ratios were calculated from the measured $Fe_2O_3^T$ and FeO values. The error on the FeO analyses is lower than 0.2 wt.% (2sd) based on repeated analyses of CRPG UB-N serpentinite standard. The method has been tested by Debret et al. (2015), who were able to match measured bulk $Fe^{3+}/\Sigma Fe$ ratios with those recalculated from μ-XANES measurements of serpentine minerals (see Debret et al., 2015 for method details, including standards, precision and calibration data for XANES measurements). Reference material values for UB-N (FeO = 2.96 wt.%) agree with previous studies (e.g., Amonette and Scott, 1991; $FeO_{(UB\text{-}N)}$ = 3.01 wt.%).

3.2. Trace elements and Fe stable isotopes

For trace elements and Fe stable isotope analyses, bulk rock samples and mineral separates were dissolved following the procedure of Debret et al. (2021). 50 mg of whole rock powders were dissolved using a 50:50 mix solution of concentrated HF and HCl acids in 7 mL PTFE Teflon square digestion vessels with wrench top closures in an oven at 160 °C for 3 days. After evaporation at 90 °C, residues were put in Aqua Regia and heated at 130 °C for 24 h. After an extra step of evaporation at 90 °C, 1 mL of HCl 6 N was added to the samples, the solution being heated at 90 °C during 24 h. This step was then reiterated, the same solution was then used for both trace element and stable isotope procedures.

3.2.1. Trace elements

For trace elements, the solutions were diluted by a factor 10 000 in HNO_3 acid. Analyses were then carried using an Agilent 7900 quadrupole ICP-MS. Elements with masses between that of sodium (23) and arsenic (75), as well as silver (107), cadmium (111) and gadolinium (157), were measured using a collision-reaction cell with helium gas (5 mL/min) to remove polyatomic interferences. All other elements were measured without collision gas. UB-N CRPG serpentinite was used as external standard. The obtained values are in good agreement with literature data (Appendix A).

3.2.2. Iron stable isotopes

Quantitative purification of Fe was achieved by chromatographic exchange, using 1 ml of AG1-x8 (200–400 mesh) and 1.2 mL Bio-Spin© chromatography columns, following the procedure developed by Sossi et al. (2015). All reagents used in the chemistry and mass spectrometry procedures were distilled and subboiled using Teflon two-bottle stills at the IPGP. The total procedural blank contribution was <80 ng of Fe, which is negligible compared to the amount of Fe in the samples (blank contribution is <<1%).

Iron isotope analyses were performed by multiple-collector inductively-coupled-plasma mass-spectrometry (MC-ICP-MS; Thermo Scientific Neptune Plus) at the IPGP. Instrumental mass fractionation was corrected using the sample-standard bracketing technique. Solutions consisted of 3 ppm natural Fe in 0.5 M HNO_3, which were introduced into the mass spectrometer using a quartz cyclonic spray chamber and PFA 100 μl/min nebulizer. The international Fe isotope standard IRMM014 was used as both the bracketing and delta notation reporting standard. To resolve the polyatomic interferences $^{40}Ar^{14}N^+$, $^{40}Ar^{16}O$ and $^{40}Ar^{16}OH^+$ that occur on masses ^{54}Fe, ^{56}Fe and ^{57}Fe, respectively, the instrument was run in high-resolution mode, which gave a mass resolving power (mass/Δmass) of ~12,000. The standard Fe beam intensities typically varied between 15 and 20 V for ^{56}Fe using a 10^{10} Ω resistor. Data were collected in 15 cycles of 8.388 second integrations. Mass dependence, long-term reproducibility, and accuracy were evaluated by analysing an in-house $FeCl_2$ salt standard. The values obtained for repeated measurements of this standard solution yielded average $\delta^{56}Fe$ values of −0.71 ± 0.04 ‰ and $\delta^{57}Fe$ values of −1.04 ± 0.13 ‰ 2sd, n = 33. These average values are in excellent agreement with previous measurements (Williams and Bizimis, 2014) and with long term measurements at IPGP ($\delta^{56}Fe = -0.73 \pm 0.05$ ‰; $\delta^{57}Fe = -1.08 \pm 0.12$ ‰, n = 122). The international rock reference materials USGS BHVO-2 (basalt) and CRPG UB-N (serpentinite) were analysed in the same analytical sessions as the samples, yielding $\delta^{56}Fe$ and $\delta^{57}Fe$ values in good agreement with literature (Appendix B).

4. Results

The results of meta-serpentinite whole rock analyses are reported in Appendix A and B and illustrated in Figs. 3 to 5. Meta-serpentinites from both the southern and northern sections of the Monviso massif have similar major element contents, aligning with the mantle terrestrial array (Fig. 3a). The Al_2O_3 and MgO contents of meta-serpentinites range from 0.3 to 2.8 wt% and from 35.2 to 43.0 wt.%, respectively, and $Fe^{3+}/\sum Fe$ ranging from 0.2 to 0.6 (Fig. 3b-c). Notably, the basal serpentinites from the Northern part display the highest $Fe^{3+}/\sum Fe$ ratios (Fig. 3c). These values are consistent with those reported in the literature (Angiboust et al., 2014; Debret et al., 2016; Gilio et al., 2020; Hattori and Guillot, 2007).

The REE patterns of the meta-serpentinites exhibit variability passing from Southern to Northern Monviso (Fig. 4). Southern meta-serpentinites are characterized by a flat Light (L) and Mid (M) REE segment (La/Sm_N = 0.8–1.9; N: Chondrite normalized, values from Barrat et al. (2012)) with a slight enrichment in Heavy (H) REE (La/Yb_N = 0.2–0.9; Gd/Yb_N = 0.4–0.6) and a negative Eu anomaly (Eu/Eu* = 0.4–0.7; Fig. 4c). Two main types of REE patterns were observed in northern meta-serpentinites (Fig. 4a-b). Meta-serpentinites sampled at the Colle Armoine (Fig. 4b) display a strong LREE depletion (La/Sm_N = 0.03–0.35; La/Yb_N = 0.03–0.21) and a relatively flat M-HREE segment (Gd/Yb_N = 1.1–1.3). REE patterns of meta-serpentinites sampled further North of this area (Fig. 4a) are similar to that of southern meta-serpentinites. They display a flat L-MREE segment (La/Sm_N = 0.9–1.3) and a slight enrichment in HREE (La/Yb_N = 0.2–0.9; Gd/Yb_N = 0.2–0.4). The olivine vein (sample VIS20–11 V) is characterized by high LREE/HREE ratio (La/Yb_N = 1.6) relative to the serpentinite host rock (Fig. 4a). Extended trace element patterns of Monviso meta-serpentinites are characterized by an alkali enrichment relative to LREE (Cs/La_n = 0.2–71, n: normalized to primitive mantle, values from Sun and McDonough (1989)), and positive Pb (Pb/Ce_n = 1.3–366), B, As and Sb anomalies relative to neighbouring elements. It must be noted that Monviso meta-serpentinites display highly variable Sr (Sr/Sr* = 0.1–7.3; $Sr^* = (Pr_n + Nd_n)/2$) and Li (Li/Li* = 0.1–10; $Li^* = (Dy_n + Y_n)/2$) anomalies (Fig. 4d-f).

The Monviso meta-serpentinites display a significant range of $\delta^{56}Fe$ values (from −0.20 ± 0.05 to +0.09 ± 0.03 ‰) relative to the primitive mantle and their variance is outside that of abyssal peridotites (Fig. 5). No systematic variations were observed passing from southern meta-serpentinites ($\delta^{56}Fe$ = −0.09 ± 0.02– +0.07 ± 0.02 ‰) to northern meta-serpentinites ($\delta^{56}Fe = -0.20 \pm 0.05$– +0.09 ± 0.03 ‰), except that the latter display a larger range of $\delta^{56}Fe$ values. These values agree with previous analyses of Western Alps HP-serpentinites (Fig. 5). Both bulk metamorphic veins ($\delta^{56}Fe = -0.19 \pm 0.05$ ‰) and magnetite separates ($\delta^{56}Fe$ = +0.10 ± 0.07– +0.15 ± 0.06 ‰) are characterized by isotopically light values relative to their abyssal pendant (Fig. 5).

5. Discussion

The studied meta-serpentinites record a complex metamorphic history, being formed in a slow spreading like environment and subsequently experienced HP-HT metamorphism during subduction, followed by exhumation through alpine orogeny (Agard (2021) and reference therein). The geochemical characteristics of the studied samples may therefore reflect various processes including (1) multiple events of partial melting and/or melt/rock interactions beneath the oceanic ridge,

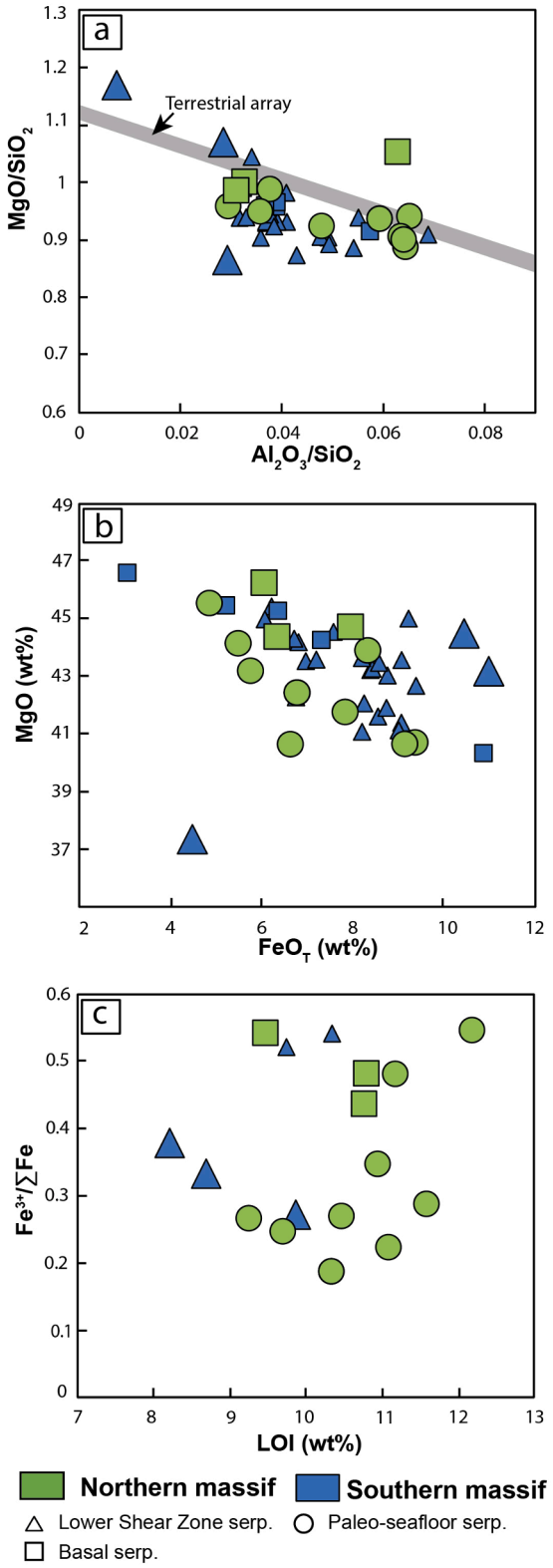

Fig. 3. Bulk rock major element composition of Monviso meta-serpentinites illustrated in (a) Al_2O_3/SiO_2 vs MgO/SiO_2, (b) FeO (wt.%) vs MgO (wt.%) and (c) Loss On Ignition (LOI, wt%) vs $Fe^{3+}/\sum Fe$. On Fig. 2a, the dark line represents the silicate Earth differentiation trend (Paulick et al., 2006). Small symbols: literature data from Hattori and Guillot (2007), Angiboust et al. (2014), Debret et al. (2016) and Gilio et al. (2020).

(2) fluid/rock interactions associated with peridotite serpentinization near the seafloor and/or (3) metamorphic processes associated with alpine subduction or collision. Hence prior to evaluating the significance of Monviso meta-serpentinite in the context of subduction zones, we first investigate the potential effects of high-temperature petrogenetic processes and seafloor hydrothermal alteration that might have modified the studied serpentinites before subduction.

5.1. *Melt-rock interactions and mantle geochemical inheritances*

The composition of mantle peridotites is commonly assessed through major element compositions with fertile lherzolites displaying high Al_2O_3, CaO and low MgO contents compared to refractory harzburgite or dunite (Bodinier and Godard, 2013). However, during the serpentinization process, both Ca and Mg can be mobilized in fluids (Deschamps et al., 2013; Paulick et al., 2006; Snow and Dick, 1995), while Al is often considered to be less mobile (Malvoisin, 2015). In addition, Paulick et al. (2006) considered Al_2O_3/SiO_2 to be a better proxy of peridotite protolith composition than Al_2O_3 concentrations as the Al_2O_3/SiO_2 ratio remains relatively unchanged during the serpentinization process, whereas Al_2O_3 concentrations can be influenced by volume changes accompanying serpentinite formation. Major elements mobility is well illustrated in Fig. 3a, where most of the studied sample follow the terrestrial Al_2O_3/SiO_2 evolution and are slightly shifted towards low MgO/SiO_2 (Fig. 3a). There is a large overlap of Al_2O_3/SiO_2 ratios between Monviso meta-serpentinites, with most of the samples spreading between a harzburgite refractory endmember with low Al_2O_3/SiO_2 ratios and a fertile lherzolite endmember with high Al_2O_3/SiO_2 ratios.

The REE patterns are variable at massif scale by presenting highly variable LREE depletion relative to M-HREE (Fig. 4). This variability is well illustrated in the Northern part of the massif where two main types of REE patterns were observed. In contrast, few variations were observed between the REE patterns of LSZ- and basal serpentinites in the southern part of the massif, either in this or in previous studies (Gilio et al., 2020). The LREE mobility can be influenced by both melt or fluid rock interactions occurring either at abyssal stage or during subduction. Notably, several studies of Western Alps meta-ophiolites (e.g., Lanzo massif) have shown that impregnation processes by MORB-like melts occurring prior subduction can generate peridotites with variable LREE enrichments relative to M-HREE (Piccardo et al., 2007). Additionally, Paulick et al. (2006) noted that the addition or removal of melts in peridotites leads to enrichments in HFSE and LREE, while LREE are more readily transported than HREE or HFSE in aqueous fluids. Hence melt/rock interactions can fractionate both LREE/HREE and HFSE ratios while fluid/rock interaction primarily affect LREE/HREE ratios. In Fig. 6a, we observed a negative correlation between La/Yb_N and Zr/Ta_n ratios in Monviso serpentinites suggesting that the observed REE patterns mainly reflect melt/rock interactions affecting peridotite prior the subduction process.

The studied samples display large $\delta^{56}Fe$ (from −0.20 to +0.09 ‰) variations relative to the reported values for fresh mantle peridotites of Balmuccia massif (Western Alps, from −0.03 to +0.06‰, Sossi et al. (2016) or abyssal peridotites (Fig. 5). It must be noted that some variations of $\delta^{56}Fe$ values can be reported across geological settings for mantle peridotites (e.g., Poitrasson et al., 2013), however, the Balmuccia peridotites are unaffected by alpine subduction or orogeny and are therefore considered as a robust value for pristine Thetys mantle (Sossi et al., 2016). An important question to address is whether the observed $\delta^{56}Fe$ variations can be inherited from melt-rock interactions during (i) partial melting and/or (ii) melt impregnation (i.e. metasomatism) occurring prior to subduction.

Previous studies have shown that the $\delta^{56}Fe$ values of peridotites can be influenced by melting, with lherzolites displaying high $\delta^{56}Fe$ values relative to harzburgite or dunite (Williams et al., 2004; Weyer and Ionov, 2007). TiO_2 concentrations increase with peridotite fertility, while FeO concentrations are little affected (Bodinier and Godard,

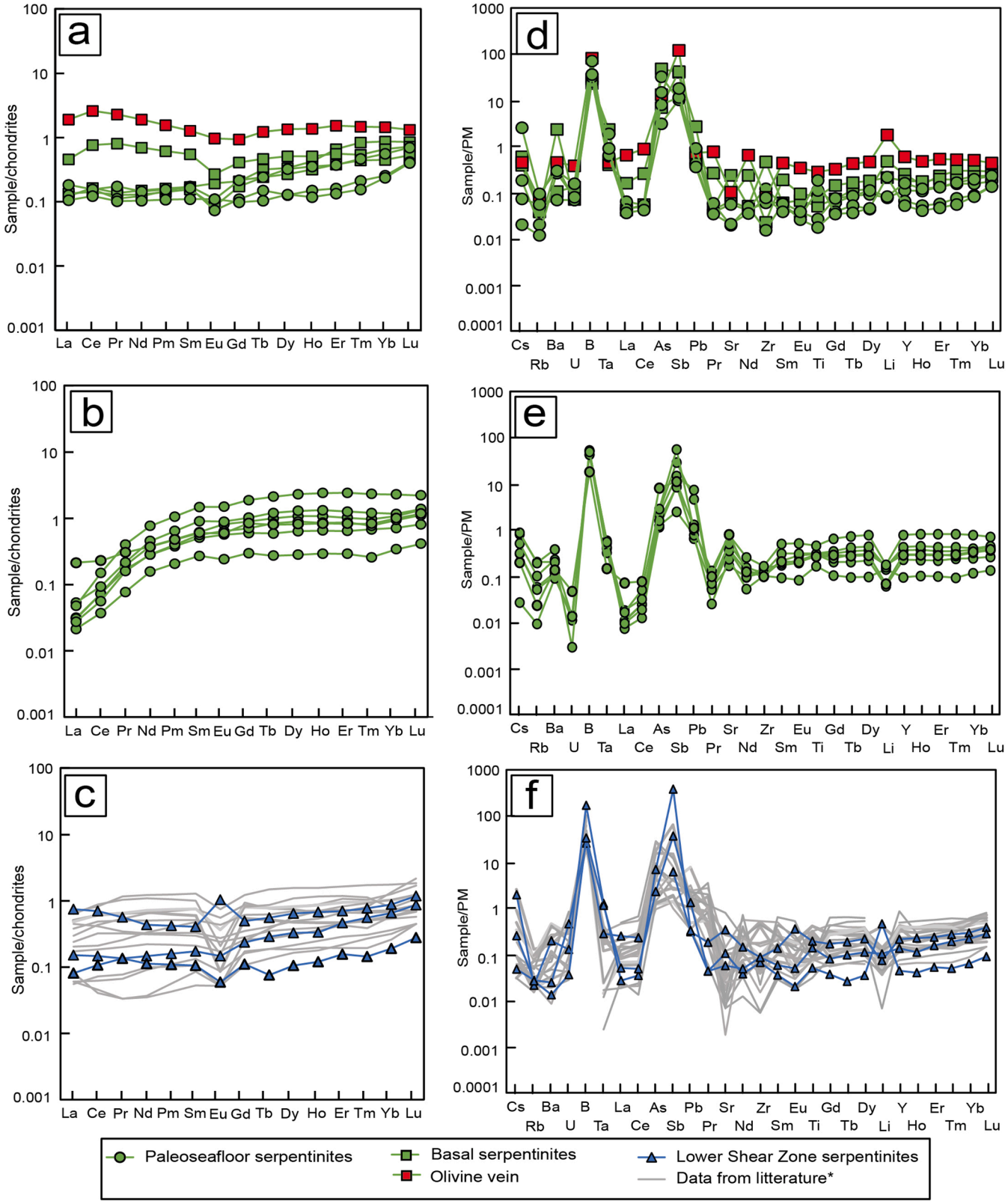

Fig. 4. Bulk rock (a-c) REE and (d-f) trace element patterns of Monviso meta-serpentinites. Literature data are from Hattori and Guillot (2007), Angiboust et al. (2014), Debret et al. (2016) and Gilio et al. (2020).

2013). Peridotite melting can thus potentially produce a negative correlation between δ^{56}Fe and Fe/Ti ratios, such as the one observed in Monviso meta-serpentinites (Fig. 6b). However, it must be noted that compared to abyssal peridotites with similar Ti concentrations, the studied samples are systematically shifted toward lighter δ^{56}Fe values. In addition, the meta-serpentinites from the Monviso massif display weak negative and positive correlations between δ^{56}Fe and La/Yb_N or Zr/Tan ratios (R^2= 0.3), respectively. In order to evaluate the possible

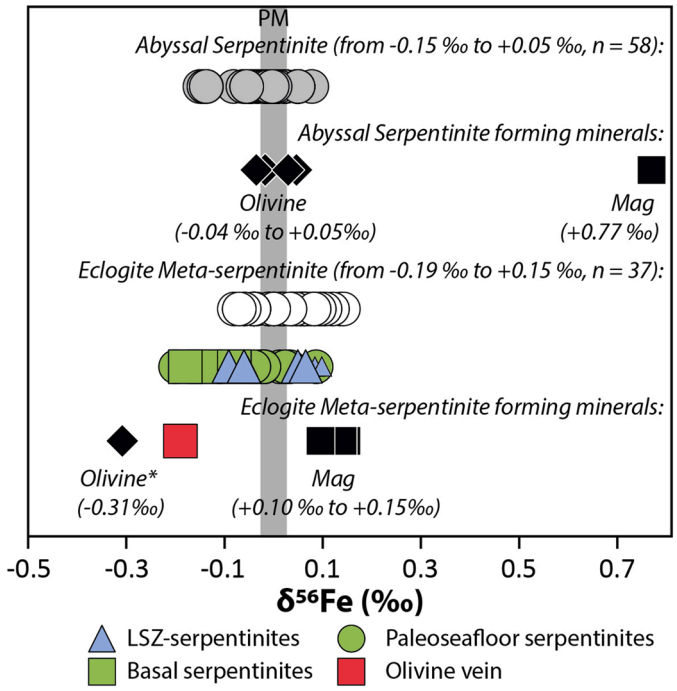

Fig. 5. Iron isotope composition (δ^{56}Fe) of serpentinites rocks composing the abyssal (grey symbol) and eclogitic (white and colour symbols) lithosphere. Separate olivine and magnetite are also display for comparison (black symbols). Colour symbols correspond to Monviso samples (this and (Debret et al., 2016) studies). Literature data are from: Abyssal serpentinites, (Craddock et al., 2013; Debret et al., 2018); Eclogite meta-serpentinites, (Debret et al., 2021, 2016). PM: Primitive mantle (Craddock et al., 2013).

influence of protolith composition on observed geochemical trends, we used the non-modal batch melting models developed by Shaw (1970) and Sossi and O'Neill (2017) for, respectively, trace element and Fe isotope partitioning during peridotite partial melting (see Appendix C for model details and *melt-mineral* fractionation factors). These models predict a decrease of La/Yb_N and an increase of Zr/Ta_n ratios in residual peridotites through partial melting, with the entire dataset being modelled with a partial melting degree comprise between 0 and 25% (Fig. 6a). The modelling also predicts a decrease of δ^{56}Fe during partial melting in agreement with MORB composition which display isotopically heavy composition relative to mantle peridotites (+0.09 ‰ to +0.18 ‰; Teng et al., 2013). However, we find that the isotopic composition of peridotite is minimally affected by melting processes (up to 0.03‰ lighter at $f = 0.3$), a result in good agreement with previous studies (e.g., Nebel et al., 2015; Dauphas et al., 2017; Sossi et al., 2018). This reflects that most of the Fe remains in the source, limiting the amount of Fe isotope fractionation that can develop in the peridotite residue (Appendix C). Therefore, the models provide an adequate description of La/Yb_N and Zr/Ta_n variations, but fail to reproduce the range of δ^{56}Fe values in the studied samples. A similar observation was reported by Dauphas et al. (2017) who suggested that the used isotope fractionation coefficients between melt and minerals are not well enough documented to predict the full extent of Fe isotope fractionation during partial melting. Despite this, these results can be used to predict the direction of co-variation between trace elements and Fe isotopes during partial melting (Fig. 6c-d). According to these models, partial melting should lead to negative and positive correlations between δ^{56}Fe versus La/Yb_N or Zr/Ta_n respectively (red curves in Fig. 6c-d). This is the opposite to what is observed in Monviso meta-serpentinites. Hence, the origin of light Fe signatures, with values down to −0.19 ‰, and high Fe/Ti ratios relative to DMM (Fig. 6b) cannot be explained by partial melting, as such processes do not generate strongly fractionated residues and are incompatible with the trace element signature of the studied samples (Fig. 6c-d).

Another scenario that may explain the Fe isotope variation observed in the Monviso meta-serpentinites is the possibility of melt impregnation. Addition of melts during peridotite exhumation in Ocean-Continent-Transition are commonly described in alpine ophiolites (e.g., Müntener et al., 2004; Piccardo et al., 2007). Given that MORB display high δ^{56}Fe values relative to DMM (Teng et al., 2013), such a process should shift peridotite composition towards heavier values, which is opposite to observations (Fig. 6b). We conclude that a melt impregnation hypothesis is not supported by our data, and that the most straightforward scenario is to consider that the light values of meta-serpentinites reflect a mobility of Fe during (de)serpentinization processes accompanying either the hydration of peridotites at the seafloor and/or the dehydration of serpentinites during subduction.

5.2. *Deciphering the geochemical imprint of abyssal versus subduction related serpentinization*

Serpentinization processes are associated with an important storage of fluid mobile elements (FME: As, Sb, B, Li, Pb, U), increasing by several orders of magnitude their concentrations relative to mantle peridotites (Deschamps et al., 2013). Peters et al. (2017) recently reported different FME enrichment trends between abyssal and forearc serpentinization environments. These trends are driven by a strong U uptake at mid-oceanic ridges, and negligible U and significant Cs enrichment in forearc environments. These contrasting geochemical behaviours are expected to be controlled by oxidising seawater rich fluids at mid-oceanic ridges and slab-modified fluids in subduction contexts. In Fig. 7, Monviso serpentinites plot below primitive mantle values, with Li/Cs, Rb/Cs, and U/Cs ratios resembling to forearc compositions. Indeed, although the massif has undergone substantial ocean floor hydration, several studies (Angiboust et al., 2014; Gilio et al., 2020) have shown that Monviso meta-serpentinites retain geochemical and isotopic (Sr, Pb) enrichments comparable to that observed in other Alpine HP meta-serpentinite (e.g., Queyras, Voltri and Cima di Gagnone), which have been related to interaction with slab derived fluids along the subduction interface during meta-ophiolite detachment from the alpine slab (Cannaò et al., 2015; Lafay et al., 2013; Scambelluri et al., 2019). It is therefore likely that the FME signature of Monviso serpentinites was overprinted by subduction related fluid /rock interactions.

Abyssal serpentinization has limited effects on the δ^{56}Fe values of mantle peridotites. Indeed, several studies have shown that abyssal serpentinite δ^{56}Fe values are close to those of primitive mantle, while no systematic δ^{56}Fe variation were observed with increasing serpentinization degree at mid-oceanic ridges (Craddock et al., 2013; Scott et al., 2017; Debret et al., 2018a) or in orogenic settings (Debret et al., 2016). This is well illustrated on Fig. 8a, where $Fe^{3+}/\sum Fe$ values of abyssal peridotites, which are known to increase during abyssal serpentinization, are uncorrelated with δ^{56}Fe values, either at global or massif scales. This reflects the low Fe concentration of seawater and a retention of initial peridotite bulk Fe concentrations and isotope compositions during the serpentinization process. Despite this, Fe isotope thermometry applied to mineral phases within abyssal peridotites reveals two distinct temperatures of equilibration. The mantle olivine and pyroxene that preserve low $\Delta^{56}Fe_{Ol\text{-}Px}$ (<0.1 ‰) corresponding to high temperature of equilibrium (1325 °C), and serpentinite assemblages that display high $\Delta^{56}Fe_{Mgt\text{-}Serp}$ (~ 0.8 ‰) corresponding to much lower temperature of equilibration (335 °C; Scott et al., 2017).

Subduction related serpentinization of Monviso meta-serpentinites is accompanied by notable Fe isotope variations (~ 0.3 ‰; Fig. 5). These variations are larger than those observed in mantle peridotites or abyssal serpentinites (~ 0.2 ‰). Furthermore, relatively low $\Delta^{56}Fe_{Mgt\text{-}Ol}$ (~ 0.4 ‰) were estimated based on magnetite mineral separate and bulk rock analyses of olivine bearing metamorphic veins (see Appendix D for calculations). These values contrast with the high $\Delta^{56}Fe_{Mgt\text{-}Ol}$ observed

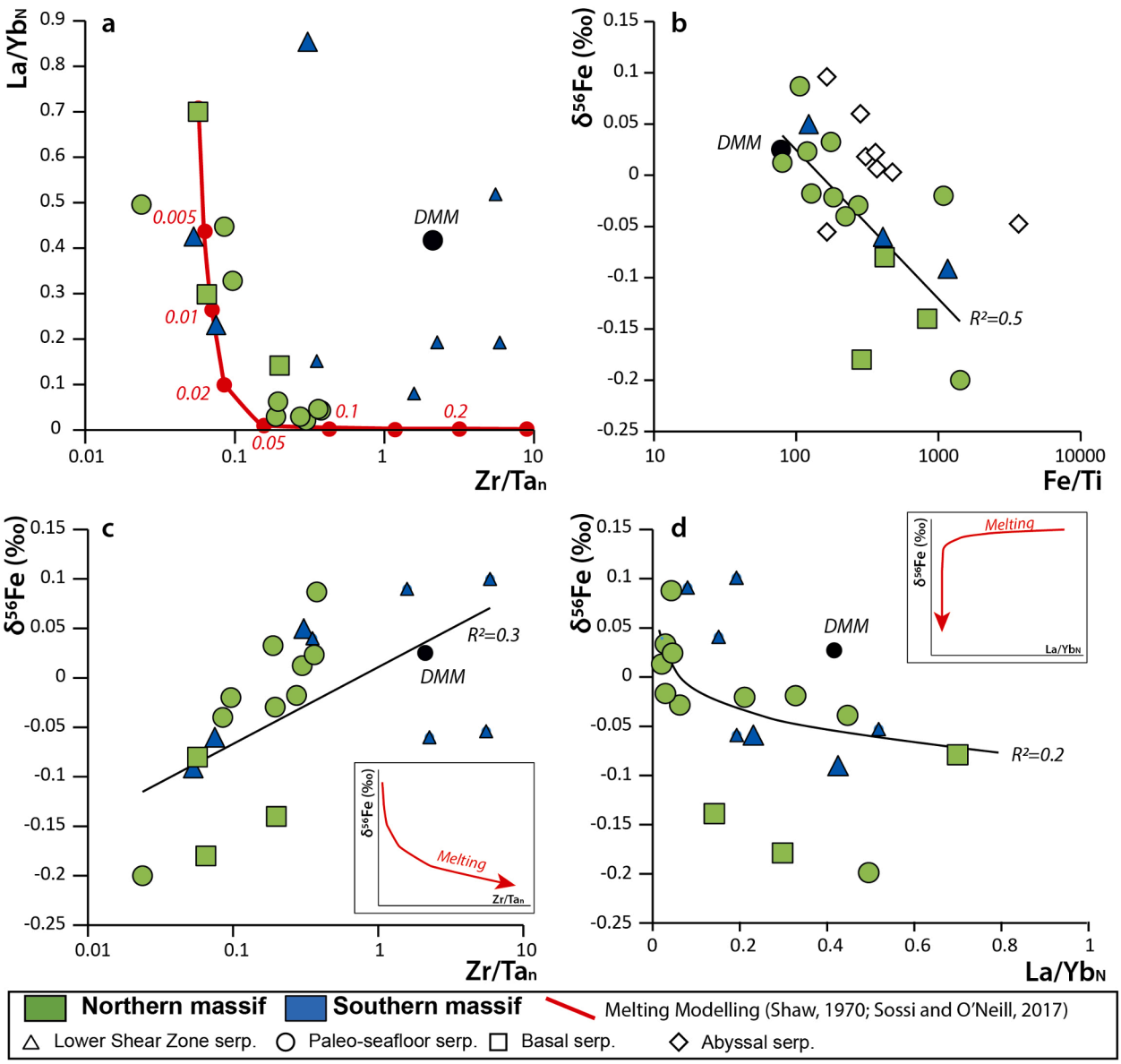

Fig. 6. Plots of (a) La/Yb_N vs Zr/Ta_n, δ56Fe vs (b) Fe/Ti, (c) Zr/Ta_n and (d) La/Yb_N ratios in meta-serpentinites. Small symbols: data from Debret et al. (2016) of Atg- and Ol-bearing serpentinites from the Monviso massif. Fe/Ti ratios were calculated from major element FeO (wt%) and trace element Ti (ppm) concentrations. The DMM values are from Salters and Stracke (2004) and Craddock et al. (2013), abyssal peridotites values are from Day et al. (2017) and Craddock et al. (2013) for trace elements and Fe isotope values, respectively. The red arrows predict the direction of co-variation between trace elements and Fe isotopes during partial melting based on geochemical modelling.

in abyssal serpentinites ($\Delta^{56}Fe_{Mgt\text{-}Ol} \sim 0.8$) and are coherent with temperature of crystallization ranging from 530 to 550 °C based on Sossi and O'Neill (2017) and Rabin et al. (2021) magnetite-olivine thermometers, respectively. These temperature estimates overlap with the metamorphic peak temperatures of Monviso meta-ophiolite (520–570 °C and 2.6–2.7 GPa; Caurant et al., 2023 and reference therein) suggesting that the observed Fe isotope variations reflect HP-HT metamorphic process related to subduction.

The observed $\delta^{56}Fe$ variation in meta-serpentinites are negatively correlated with $Fe^{3+}/\sum Fe$ ratios at massif scale (Fig. 8b), with basal serpentinites displaying low $\delta^{56}Fe$ and high $Fe^{3+}/\sum Fe$ ratios relative to paleaoseafloor serpentinites. Such type of correlation is absent in abyssal serpentinites, at either local or global scales (see discussion above, Fig. 8a). This is therefore suggestive of a Fe mobility in metamorphic fluids during subduction. The later can be attributed to either a gain or a loss of isotopically light or heavy Fe, respectively. Such a process can be driven by factors such as (1) variations in Fe oxidation state controlling equilibrium Fe isotope fractionation between solids and/or fluids, and/or (2) non-redox attributes such as ligands present in the aqueous solution.

In the Northern Monviso, meta-serpentinites were intensively dehydrated through brucite breakdown during subduction (Caurant et al., 2023). This dehydration process resulted in large redox variations, with paleo-seafloor serpentinites being equilibrated at fO_2 as low as FMQ −4 and basal serpentinites being equilibrated as high as FMQ +2. These redox variations directly affected the distribution of Fe between HP-phases, with basal serpentinites displaying abundant magnetite and high $Fe^{3+}/\sum Fe$ (0.48–0.56) relative to paleo-seafloor (0.19–0.54) serpentinites (Fig. 3c). The highest $Fe^{3+}/\sum Fe$ values correspond to a large metamorphic vein (sample VIS20–11 V). These redox variations are negatively correlated with $\delta^{56}Fe$ values in meta-serpentinites (Fig. 8b), suggesting a direct link between the fO_2 record of meta-serpentinites and their Fe isotope signature. It must be noted that this correlation is less pronounced in the Southern Monviso where serpentinites do not

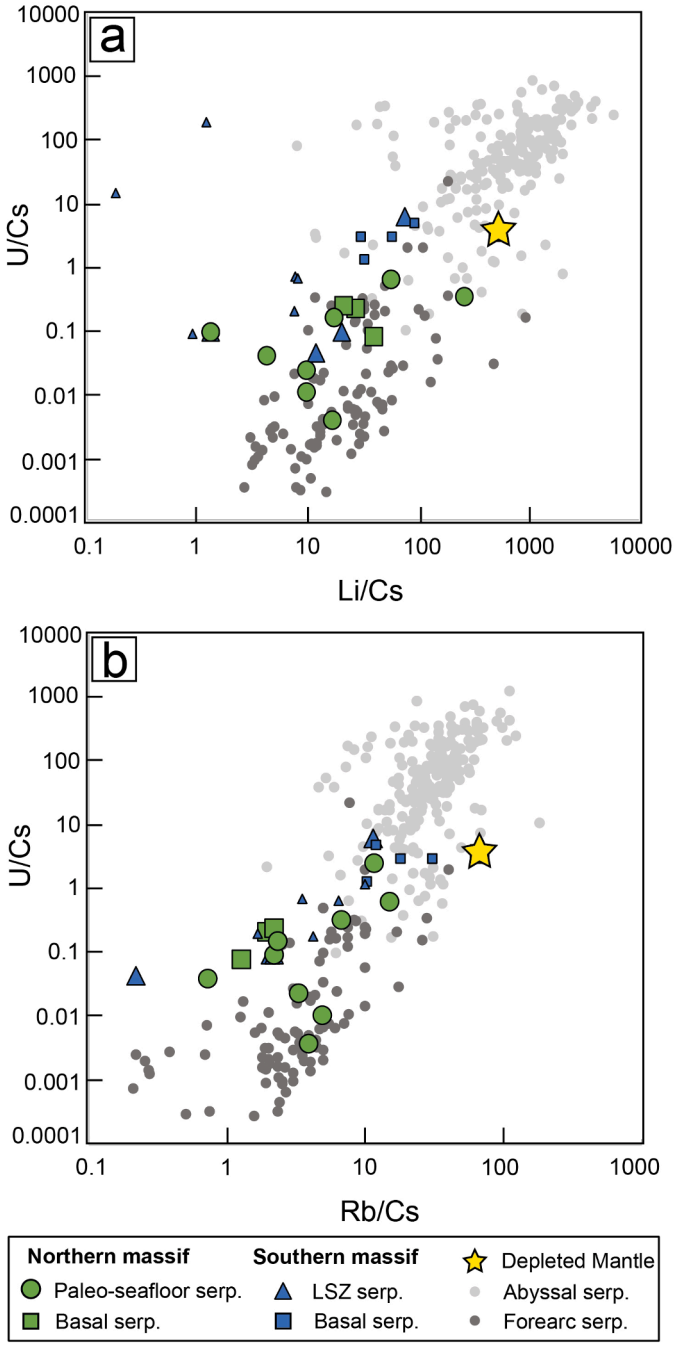

Fig. 7. Element ratio discrimination for mid ocean ridge and forearc serpentinites (data from Peters et al., 2017). Plots of U/Cs vs (a) Li/Cs and (b) Rb/Cs for ultramafic rocks composing Monviso and massif.

always display dehydration features (e.g., metamorphic olivine, Gilio et al., 2020), while one sample from paleo-seafloor serpentinites with high LOI (11.2 wt%) display abnormally high $Fe^{3+}/\sum Fe$ and $\delta^{56}Fe$ (Vis18–6A). In fact, Debret et al. (2014) already noted that olivine-bearing serpentinites (i.e., meta-serpentinites) display lower $Fe^{3+}/\sum Fe$ relative to antigorite-bearing serpentinites. This was attributed to the formation of Fe^{3+}-rich antigorite, with $Fe^{3+}/\sum Fe$ as high as 0.5, that controls the Fe redox budget of serpentinite prior their dehydration. The presence of abundant Fe^{3+}-antigorite in the less dehydrated samples might therefore scatter the use of $Fe^{3+}/\sum Fe$ as an approximation for magnetite formation in the studied samples, explaining the outliners in the Fig. 8b. Here, we further investigate the factors influencing the redox and isotopic variations in meta-serpentinites.

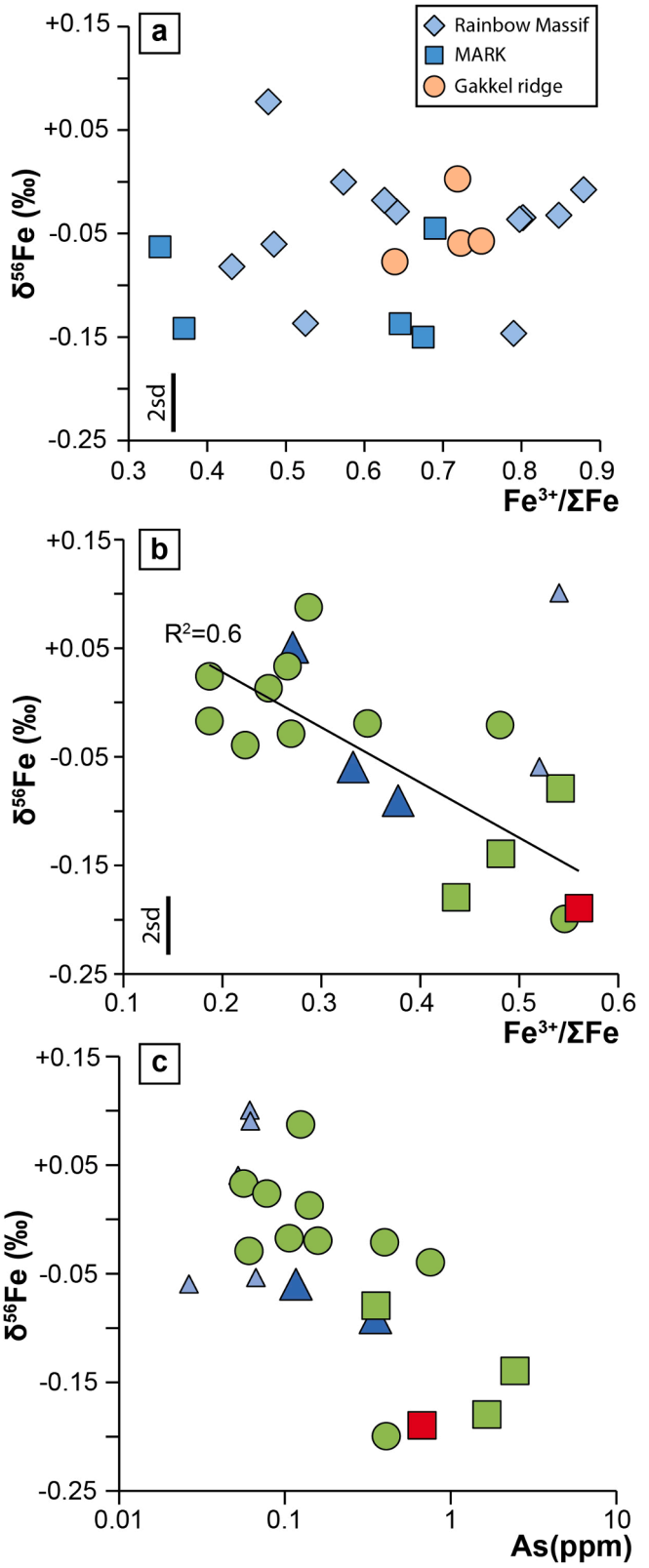

Fig. 8. Bulk rock $\delta^{56}Fe$ (‰) versus (a-b) $Fe^{3+}/\sum Fe$ and (c) As (ppm) variations in abyssal serpentinites (data from Debret et al., 2018) and Monviso meta-serpentinites. Small symbols are from Debret et al. (2016).

Experimental and theoretical studies predict that, at equilibrium, Fe^{2+}-bearing phases should be isotopically lighter than Fe^{3+}-bearing phases (Polyakov and Mineev, 2000) which is in apparent contradiction with the negative correlation between bulk serpentinite $\delta^{56}Fe$ and $Fe^{3+}/\Sigma Fe$ (Fig. 8b). Debret et al. (2016) reported a similar paradox in other Western Alps meta-ophiolites (e.g., Lanzo or Queyras massifs) and proposed that this correlation should reflect the loss of an isotopically light Fe component in the form of Fe(II)-SO_x or Fe(II)-Cl complexes. According to theoretical models, these complexes should preferentially incorporate lighter Fe relative to olivine or other reduced complexes (Fujii et al., 2014). In agreement with this scenario, the metamorphic vein (sample Vis20–11 V) is characterized by the highest $Fe^{3+}/\sum Fe$ and the lightest $\delta^{56}Fe$. Given that Fe^{3+} is considered as immobile in fluids, this geochemical behaviour likely reflects the precipitation of isotopically light iron during fluid pathway closure during prograde metamorphism. This can be explained through the following redox equation (Debret et al., 2016):

$$Fe\text{-}SO_{4(aq)} + 12FeO = 4Fe_3O_4 + FeS \quad (1)$$

This is consistent with thermodynamic modelling predicting a high fO_2 (FMQ +2) and magnetite formation during the dehydration of basal serpentinites at HP-HT (Caurant et al., 2023). Interestingly, only samples equilibrated at high fO_2 and displaying high $Fe^{3+}/\sum Fe$ seem to display fractionated Fe isotope values, while samples equilibrated at lower fO_2 conditions and displaying low $Fe^{3+}/\sum Fe$ display mantle like values (Fig. 8b). The observation of isotopically light veins with high $Fe^{3+}/\sum Fe$ in basal serpentinites suggests that the fO_2 was imposed by external fluids percolating the massif rather than mineral reactions accompanying serpentinite dehydration at high pressure. In agreement with such a scenario, the observed $\delta^{56}Fe$ variations are negatively correlated with Fe/Ti ratios (Fig. 6b). Titanium is usually consider as immobile in aqueous fluids. However, the observed correlation between $\delta^{56}Fe$ and Fe/Ti is rather driven by small variations in Ti concentrations (between 100 and 600 ppm in the studied samples) rather than Fe contents, the latter being a major element. Experimental studies have shown that whereas TiO_2 solubility in pure H_2O is quite low (ppm range), it increases by orders of magnitude upon addition of chlorine and fluorine ligands in fluids (Rapp et al., 2010; Tanis et al., 2016). It is therefore plausible that the correlation between $\delta^{56}Fe$ and Fe/Ti reflect a mixing process between a fluid, with isotopically light Fe signature and high Fe/Ti ratio, and a mantle-like endmember. The percolation of oxidising fluids is also coherent with a correlation between $\delta^{56}Fe$ and As concentrations in meta-serpentinites. Arsenic is a FME that can display contrasting redox speciation, with reduced arsenide (As–III) being less mobile than arsenite (AsIII) and arsenate (AsV). It has been shown that oxidative dissolution of arsenide should favour a high mobility of As in metamorphic fluids during subduction (Pokrovski et al., 2022). Although we did not specifically determine the arsenic redox and structural state in the studied samples, it is noteworthy that samples equilibrated at higher fO_2 values, and displaying the lightest $\delta^{56}Fe$ values, also have the highest As content, as shown by the metamorphic veins (Fig. 8c). In contrast, isotopically heavy Fe and Fe^{3+}-poor serpentinites display the lowest As contents. These covariations between Fe redox state, isotopes and As contents further support a high mobility of As under oxidising form during the percolation of fluids in the massif.

Based on structural, petrological and geochemical observations, previous studies proposed that the Monviso massif is a section of oceanic lithosphere that was subducted and then exhumed along the subduction interface (Agard, 2021; Angiboust et al., 2014, 2012; Locatelli et al., 2019b, 2018). The detachment of the Monviso from the alpine slab occurred at eclogite facies P-T conditions as shown by the presence of eclogite brecciation along major shear zones (Angiboust et al., 2011; Fig. 9). The percolation of oxidising fluids must be concomitant to this event since the temperature equilibration between olivine and magnetite are close to that of Monviso P-T climax. External fluid circulations within the massif are favoured nearby major detachment structures, such as the basal units, which must have suffered more intense metasomatism than paleoseafloor lithologies. Although we did not identify the source of the fluid here, Angiboust et al. (2014) report heavy boron isotope signature in eclogite forming minerals from the LSZ. Such isotopic signature represents a well-established maker of serpentinite derived fluids in subduction zones (Scambelluri and Tonarini, 2012).

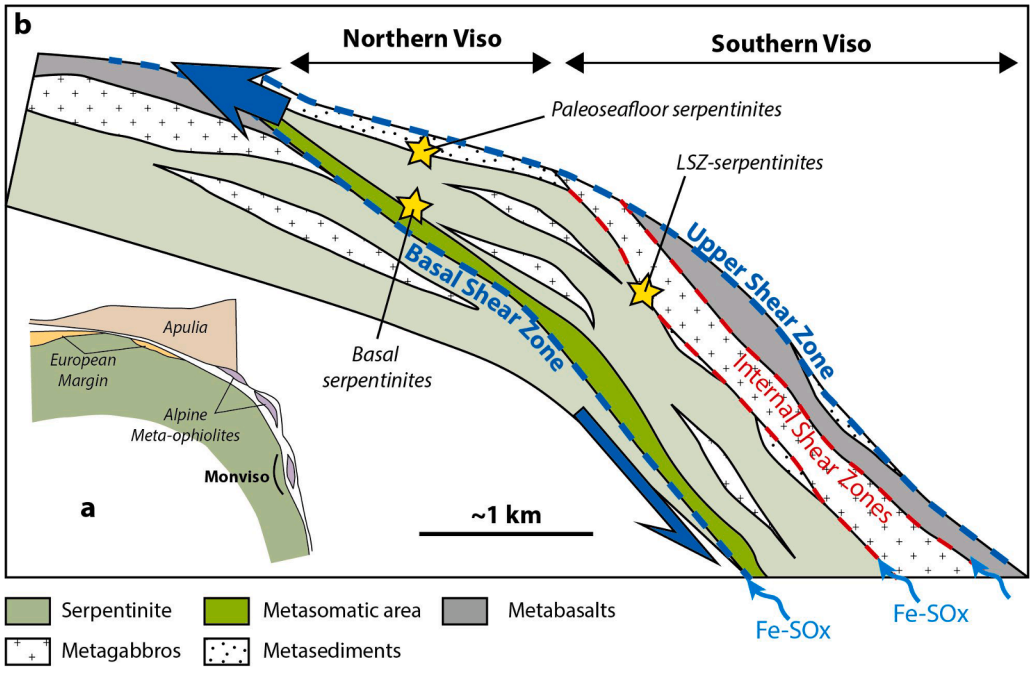

Fig. 9. Detachment of the Monviso and fluid migration events inside the alpine slab (modified after Locatelli et al., 2018; Agard et al., 2001). a Tectonic sketch of the alpine subduction locating meta-ophiolite detachments along the plate interface. b Idealized restoration of the Monviso detachment from the alpine slab. The shearing mainly occurred at the detachment (Basal Shear Zone) and along lithological discontinuities hence favouring the metasomatism of basal serpentinites by oxidising fluids carrying isotopically light signature (e.g., Fe-SOx).

The mobility of iron in fluids is constrained to the formation oxidising ligands, such as Fe(II)-CO_2 or Fe(II)-SO_4, that preferentially complex isotopically light Fe (Fujii et al., 2014). Among slab lithologies, it has been proposed that serpentinite dehydration could occur at fO_2 conditions (Debret and Sverjensky, 2017), favouring the mobility of isotopically light Fe in slab derived fluids (Debret et al., 2016). The heavy boron (Angiboust et al., 2014) and light iron (this study) isotope signatures in eclogite lithologies from the Monviso massif could therefore point toward a contribution of external fluids derived from serpentinite dehydration at HP-HT.

Recent geochemical studies highlight a contribution of serpentinite derived fluids to explain the oxidation state of arc magmas (e.g., Chen et al., 2023; Rojas-Kolomiets et al., 2023; Zhang et al., 2021). Those are based on systematics between boron isotopes and redox sensitive proxies in arc lavas. In particular, Chen et al. (2023) report similar variations between B and Fe isotopes as those inferred in the Monviso massif. These authors speculate that the light Fe signature of arc magmas could reflect the transfer of an oxidising component derived from slab serpentinites. In agreement with these studies, we show that fO_2 conditions have a first order control on Fe mobility during prograde metamorphic reactions, with only samples equilibrated at high fO_2 conditions recording isotopically light Fe signatures. These results therefore establish a direct link between Fe isotope signature and fO_2 record in subduction zones. To that regard, the isotopically light signature of arc magmas likely reflects the participation of an oxidising component derived from the slab serpentinite in their source.

6. Conclusions

The analysis of Monviso meta-serpentinites reveals the preservation of mantle geochemical heterogeneities inherited from an abyssal stage. This is supported by negative correlations between HFSE and LREE/HREE ratios in meta-serpentinite. Such correlation arises due to the addition or removal of melts in peridotites leading to enrichments in HFSE and LREE, while LREE are more readily transported than HREE or HFSE in aqueous fluids. However, fractional melting models failed to explain the isotopically light $\delta^{56}Fe$ signatures in meta-serpentinites.

The negligible U and prominent Cs enrichments in Monviso meta-serpentinites suggest that the meta-serpentinite FME signature was overprinted by subduction related fluid /rock interactions at HP-HT. Although some overlap remains between abyssal and Monviso (meta-) serpentinites, the existence of a negative correlation between $\delta^{56}Fe$ and $Fe^{3+}/\sum Fe$ or As contents in meta-serpentinites provides evidence for a mobility of isotopically light Fe in slab derived fluids during subduction. This observation is further supported by mineral separate analyses of olivine-bearing veins that record low $\Delta^{56}Fe_{Mgt\text{-}Ol}$, compatible with high temperatures processes associated with subduction P-T conditions. Both the observation of isotopically light veins with high $Fe^{3+}/\sum Fe$ and correlation between $\delta^{56}Fe$ and Fe/Ti ratio suggest that the observed $\delta^{56}Fe$ in HP meta-ophiolites are controlled by exchange with external fluids during prograde metamorphism.

Interestingly, these isotopic variations are directly linked to the fO_2 record of metamorphic samples, with samples equilibrated at high fO_2 displaying the most fractionated Fe isotope values. This highlights the role of redox variation accompanying metamorphic reaction on Fe mobility in subduction zones, where oxidising conditions favour the transfer of isotopically light Fe in fluids.

CRediT authorship contribution statement

Baptiste Debret: Writing – original draft, Validation, Supervision, Methodology, Funding acquisition, Data curation, Conceptualization. **Clara Caurant:** Investigation, Formal analysis, Data curation. **Bénédicte Ménez:** Conceptualization. **Vincent Busigny:** Writing – original draft, Data curation. **Frédéric Moynier:** Writing – original draft, Data curation.

Declaration of competing interest

The authors declare that they have no known competing financial interests or personal relationships that could have appeared to influence the work reported in this paper.

Data availability

Data are in appendixes.

Acknowledgments

The authors thank P. Burkel, Tutu and D. Rigoussen for their precious help during geochemical analyses and P. Sossi for his help with melting models. We thank M. Bizimis and an anonymous reviewer for critical comments on earlier version of this article and careful editorial handling by R. Hickey-Vargas. This work was supported by the Agence Nationale de la Recherche (ANR) CARBioNic "ANR-22-CE49–0001–01". Part of this work was also supported by IPGP multidisciplinary program PARI, and by Region Ile- de-France SESAME grants no. 12015908 and EX047016. FM acknowledge support from the ERC grant agreement No. 101001282 (METAL).

Supplementary materials

Supplementary material associated with this article can be found, in the online version, at doi:10.1016/j.epsl.2024.118855.

References

Agard, P., 2021. Subduction of oceanic lithosphere in the Alps: selective and archetypal from (slow-spreading) oceans. Earth-Science Rev. 214, 103517 https://doi.org/10.1016/j.earscirev.2021.103517.

Agard, P., Jolivet, L., Goffe, B., 2001. Tectonometamorphic evolution of the schistes lustres complex; implications for the exhumation of HP and UHP rocks in the Western Alps. Bull. la Société géologique Fr. 172, 617–636.

Amonette, J.E., Scott, A.D., 1991. Determination of ferrous iron in non-refractory silicate minerals. 1. An improved semi-micro oxidimetric method. Chem. Geol. 92, 329–338. https://doi.org/10.1016/0009-2541(91)90077-5.

Angiboust, S., Agard, P., Raimbourg, H., Yamato, P., Huet, B., 2011. Subduction interface processes recorded by eclogite-facies shear zones (Monviso, W. Alps). Lithos 127, 222–238.

Angiboust, S., Langdon, R., Agard, P., Waters, D., Chopin, C., 2012. Eclogitization of the Monviso ophiolite (W. Alps) and implications on subduction dynamics. J. Metamorph. Geol. 30, 37–61. https://doi.org/10.1111/j.1525-1314.2011.00951.x.

Angiboust, S., Pettke, T., De Hoog, J.C.M., Caron, B., Oncken, O., 2014. Channelized fluid flow and eclogite-facies metasomatism along the subduction shear zone. J. Petrol. 55, 883–916. https://doi.org/10.1093/petrology/egu010.

Arculus, R.J., 1994. Aspects of magma genesis in arcs. Lithos 33, 189–208. https://doi.org/10.1016/0024-4937(94)90060-4.

Balestro, G., Festa, A., Dilek, Y., Tartarotti, P., 2015. Pre-alpine extensional tectonics of a peridotite-localized oceanic core complex in the late Jurassic, high-pressure Monviso ophiolite (Western Alps). Episodes 38, 266–282. https://doi.org/10.18814/epiiugs/2015/v38i4/82421.

Balestro, G., Fioraso, G., Lombardo, B., 2013. Geological map of the Monviso massif (Western Alps). J. Maps 9, 623–634. https://doi.org/10.1080/17445647.2013.842507.

Balestro, G., Fioraso, G., Lombardo, B., 2011. Geological map of the upper pellice valley (ItalianWestern Alps). J. Maps 7, 634–654. https://doi.org/10.4113/jom.2011.1213.

Ballèvre, M., Lagabrielle, Y., Merle, O., 1990. Tertiary ductile normal faulting as a consequence of lithospheric stacking in the western Alps. Mémoires la Société géologique Fr 156, 227–236.

Barrat, J.A., Zanda, B., Moynier, F., Bollinger, C., Liorzou, C., Bayon, G., 2012. Geochemistry of CI chondrites: major and trace elements, and Cu and Zn Isotopes. Geochim. Cosmochim. Acta 83, 79–92. https://doi.org/10.1016/j.gca.2011.12.011.

Bodinier, J.L., Godard, M., 2013. Orogenic, ophiolitic, and abyssal peridotites, 3rd ed. Treatise on geochemistry: second edition. Elsevier Ltd. https://doi.org/10.1016/B978-0-08-095975-7.00204-7.

Bretscher, A., Hermann, J., Pettke, T., 2018. The influence of oceanic oxidation on serpentinite dehydration during subduction. Earth Planet. Sci. Lett. 499, 173–184. https://doi.org/10.1016/j.epsl.2018.07.017.

Brounce, M., Kelley, K.A., Cottrell, E., Reagan, M.K., 2015. Temporal evolution of mantle wedge oxygen fugacity during subduction initiation. Geology 43, 775–778. https://doi.org/10.1130/G36742.1.

Cannaò, E., Agostini, S., Scambelluri, M., Tonarini, S., Godard, M., 2015. B, Sr and Pb isotope geochemistry of high-pressure Alpine metaperidotites monitors fluid-mediated element recycling during serpentinite dehydration in subduction mélange (Cima di Gagnone, Swiss Central Alps). Geochim. Cosmochim. Acta 163, 80–100. https://doi.org/10.1016/j.gca.2015.04.024.

Carignan, J., Hild, P., Mevelle, G., Morel, J., Yeghicheyan, D., 2001. Routine analyses of trace elements in geological samples using flow injection and low pressure on-line liquid chromatography coupled to ICP-MS: a study of geochemical reference materials BR, DR-N, UB-N, AN-G and GH. Geostand. Newsl 25, 187–198. https://doi.org/10.1111/j.1751-908x.2001.tb00595.x.

Caurant, C., Debret, B., Ménez, B., Nicollet, C., Bouilhol, P., 2023. Redox heterogeneities in a subducting slab: example from the Monviso meta-ophiolite (Western Alps, Italy). Lithos 107136. https://doi.org/10.1016/j.lithos.2023.107136.

Chen, Y.X., Lu, W., He, Y., Schertl, H.P., Zheng, Y.F., Xiong, J.W., Zhou, K., 2019. Tracking Fe mobility and Fe speciation in subduction zone fluids at the slab-mantle interface in a subduction channel: a tale of whiteschist from the Western Alps. Geochim. Cosmochim. Acta 267, 1–16. https://doi.org/10.1016/j.gca.2019.09.020.

Chen, Z., Chen, J., Tamehe, L.S., Zhang, Y., Zeng, Z., Zhang, T., Shuai, W., Yin, X., 2023. Light Fe isotopes in arc magmas from cold subduction zones: implications for serpentinite-derived fluids oxidized the sub-arc mantle. Geochim. Cosmochim. Acta 342, 1–14. https://doi.org/10.1016/j.gca.2022.12.005.

Craddock, P.R., Warren, J.M., Dauphas, N., 2013. Abyssal peridotites reveal the near-chondritic Fe isotopic composition of the Earth. Earth Planet. Sci. Lett. 365, 63–76. https://doi.org/10.1016/j.epsl.2013.01.011.

Dauphas, N., Craddock, P.R., Asimow, P.D., Bennett, V.C., Nutman, A.P., Ohnenstetter, D., 2009. Iron isotopes may reveal the redox conditions of mantle melting from Archean to Present. Earth Planet. Sci. Lett. https://doi.org/10.1016/j.epsl.2009.09.029.

Dauphas, N., John, S.G., Rouxel, O., 2017. Iron isotope systematics. Non-Traditional Stable Isot 82, 415–510. https://doi.org/10.2138/rmg.2017.82.11.

Day, J.M.D., Walker, R.J., Warren, J.M., 2017. 186Os–187Os and highly siderophile element abundance systematics of the mantle revealed by abyssal peridotites and Os-rich alloys. Geochim. Cosmochim. Acta 200, 232–254.

Debret, B., Andreani, M., Muñoz, M., Bolfan-Casanova, N., Carlut, J., Nicollet, C., Schwartz, S., Trcera, N., 2014. Evolution of Fe redox state in serpentine during subduction. Earth Planet. Sci. Lett. 400, 206–218. https://doi.org/10.1016/j.epsl.2014.05.038.

Debret, B., Beunon, H., Mattielli, N., Andreani, M., Ribeiro da Costa, I., Escartin, J., 2018. Ore component mobility, transport and mineralization at mid-oceanic ridges: a stable isotopes (Zn, Cu and Fe) study of the Rainbow massif (Mid-Atlantic Ridge 36°14′N). Earth Planet. Sci. Lett. 503, 170–180. https://doi.org/10.1016/j.epsl.2018.09.009.

Debret, B., Bolfan-Casanova, N., Padrón-Navarta, J.A., Martin-Hernandez, F., Andreani, M., Garrido, C.J., López Sánchez-Vizcaíno, V., Gómez-Pugnaire, M.T., Muñoz, M., Trcera, N., 2015. Redox state of iron during high-pressure serpentinite dehydration. Contrib. to Mineral. Petrol. 169, 36. https://doi.org/10.1007/s00410-015-1130-y.

Debret, B., Garrido, C.J., Pons, M.L., Bouilhol, P., Inglis, E., López Sánchez-Vizcaíno, V., Williams, H., 2021. Iron and zinc stable isotope evidence for open-system high-pressure dehydration of antigorite serpentinite in subduction zones. Geochim. Cosmochim. Acta 296, 210–225. https://doi.org/10.1016/j.gca.2020.12.001.

Debret, B., Millet, M.A., Pons, M.L., Bouilhol, P., Inglis, E., Williams, H., 2016. Isotopic evidence for iron mobility during subduction. Geology 44, 215–218. https://doi.org/10.1130/G37565.1.

Debret, B., Sverjensky, D.A., 2017. Highly oxidising fluids generated during serpentinite breakdown in subduction zones. Sci. Rep. 7, 10351. https://doi.org/10.1038/s41598-017-09626-y.

Deng, J., He, Y., Zartman, R.E., Yang, X., Sun, W., 2022. Large iron isotope fractionation during mantle wedge serpentinization: implications for iron isotopes of arc magmas. Earth Planet. Sci. Lett. 583, 117423 https://doi.org/10.1016/j.epsl.2022.117423.

Deschamps, F., Godard, M., Guillot, S., Hattori, K., 2013. Geochemistry of subduction zone serpentinites: a review. Lithos 178, 96–127. https://doi.org/10.1016/j.lithos.2013.05.019.

El Korh, A., Luais, B., Deloule, E., Cividini, D., 2017. Iron isotope fractionation in subduction-related high-pressure metabasites (Ile de Groix, France). Contrib. to Mineral. Petrol. 172 https://doi.org/10.1007/s00410-017-1357-x.

Evans, K.A., 2012. The redox budget of subduction zones. Earth-Sci. Rev 113, 11–32. https://doi.org/10.1016/j.earscirev.2012.03.003.

Evans, K.A., Frost, B.R., 2021. Deserpentinization in subduction zones as a source of oxidation in arcs: a reality check. J. Petrol. 62, egab016. https://doi.org/10.1093/petrology/egab016.

Foden, J., Sossi, P.A., Nebel, O., 2018. Controls on the iron isotopic composition of global arc magmas. Earth Planet. Sci. Lett. https://doi.org/10.1016/j.epsl.2018.04.039.

Fujii, T., Moynier, F., Blichert-Toft, J., Albarède, F., 2014. Density functional theory estimation of isotope fractionation of Fe, Ni, Cu, and Zn among species relevant to geochemical and biological environments. Geochim. Cosmochim. Acta 140, 553–576. https://doi.org/10.1016/j.gca.2014.05.051.

Gaborieau, M., Laubier, M., Bolfan-Casanova, N., McCammon, C.A., Vantelon, D., Chumakov, A.I., Schiavi, F., Neuville, D.R., Venugopal, S., 2020. Determination of Fe3+/ΣFe of olivine-hosted melt inclusions using Mössbauer and XANES spectroscopy. Chem. Geol. 547 https://doi.org/10.1016/j.chemgeo.2020.119646.

Gerrits, A.R., Inglis, E.C., Dragovic, B., Starr, P.G., Baxter, E.F., Burton, K.W., 2019. Release of oxidizing fluids in subduction zones recorded by iron isotope zonation in garnet. Nat. Geosci. 12, 1029–1033. https://doi.org/10.1038/s41561-019-0471-y.

Gilio, M., Scambelluri, M., Agostini, S., Godard, M., Pettke, T., Agard, P., Locatelli, M., Angiboust, S., 2020. Fingerprinting and relocating tectonic slices along the plate interface: evidence from the Lago Superiore unit at Monviso (Western Alps). Lithos 352–353, 105308. https://doi.org/10.1016/j.lithos.2019.105308.

Hattori, K.H., Guillot, S., 2007. Geochemical character of serpentinites associated with high- to ultrahigh-pressure metamorphic rocks in the Alps, Cuba, and the Himalayas: recycling of elements in subduction zones. Geochem., Geophys. Geosyst. 8 https://doi.org/10.1029/2007GC001594.

Hill, P.S., Schauble, E.A., 2008. Modeling the effects of bond environment on equilibrium iron isotope fractionation in ferric aquo-chloro complexes. Geochim. Cosmochim. Acta 72, 1939–1958. https://doi.org/10.1016/j.gca.2007.12.023.

Inglis, E.C., Debret, B., Burton, K.W., Millet, M.A., Pons, M.L., Dale, C.W., Bouilhol, P., Cooper, M., Nowell, G.M., McCoy-West, A.J., Williams, H.M., 2017. The behavior of iron and zinc stable isotopes accompanying the subduction of mafic oceanic crust: a case study from Western Alpine ophiolites. Geochem., Geophys. Geosyst. 18 https://doi.org/10.1002/2016GC006735.

Kelley, K.A., Cottrell, E., 2009. Water and the oxidation state of subduction zone magmas. Science (80-.) 325, 605–607. https://doi.org/10.1126/science.1174156.

Lafay, R., Deschamps, F., Schwartz, S., Guillot, S., Godard, M., Debret, B., Nicollet, C., 2013. High-pressure serpentinites, a trap-and-release system controlled by metamorphic conditions: example from the Piedmont zone of the western Alps. Chem. Geol. 343 https://doi.org/10.1016/j.chemgeo.2013.02.008.

Lagabrielle, Y., Cannat, M., 1990. Alpine Jurassic ophiolites resemble the modern central Atlantic basement. Geology 18, 319–322. https://doi.org/10.1130/0091-7613(1990)018<0319:AJORTM>2.3.CO;2.

Lee, C.T.A., Leeman, W.P., Canil, D., Li, Z.X.A., 2005. Similar V/*Sc* systematics in MORB and arc basalts: implications for the oxygen fugacities of their mantle source regions. J. Petrol. 46, 2313–2336. https://doi.org/10.1093/petrology/egi056.

Lee, C.T.A., Luffi, P., Le Roux, V., Dasgupta, R., Albaréde, F., Leeman, W.P., 2010. The redox state of arc mantle using Zn/Fe systematics. Nature 468, 681–685. https://doi.org/10.1038/nature09617.

Locatelli, M., Federico, L., Agard, P., Verlaguet, A., 2019a. Geology of the southern Monviso metaophiolite complex (W-Alps, Italy). J. Maps 15, 283–297. https://doi.org/10.1080/17445647.2019.1592030.

Locatelli, M., Verlaguet, A., Agard, P., Federico, L., Angiboust, S., 2018. Intermediate-depth brecciation along the subduction plate interface (Monviso eclogite, W. Alps). Lithos 320–321, 378–402. https://doi.org/10.1016/j.lithos.2018.09.028.

Locatelli, M., Verlaguet, A., Agard, P., Pettke, T., Federico, L., 2019b. Fluid pulses during stepwise brecciation at intermediate subduction depths (Monviso eclogites, W. Alps): first internally then externally sourced. Geochemistry, Geophys. Geosystems 20, 5285–5318. https://doi.org/10.1029/2019GC008549.

Lombardo, B., Nervo, R., Compagnoni, R., Messiga, B., Kienast, J., Mevel, C., Fiora, L., Piccardo, G., Lanza, R., 1978. Osservazioni preliminari sulle ofioliti metamorfiche del Monviso (Alpi Occidentali). Rend. Soc. Ital. di Mineral. e Petrol. 34, 253–305.

Malvoisin, B., 2015. Mass transfer in the oceanic lithosphere: serpentinization is not isochemical. Earth Planet. Sci. Lett. 430, 75–85. https://doi.org/10.1016/j.epsl.2015.07.043.

Müntener, O., Pettke, T., Desmurs, L., Meier, M., Schaltegger, U., 2004. Refertilization of mantle peridotite in embryonic ocean basins: trace element and Nd isotopic evidence and implications for crust–mantle relationships. Earth Planet. Sci. Lett. 221, 293–308.

Nebel, O., Sossi, P.A., Bénard, A., Wille, M., Vroon, P.Z., Arculus, R.J., 2015. Redox-variability and controls in subduction zones from an iron-isotope perspective. Earth Planet. Sci. Lett. 432, 142–151. https://doi.org/10.1016/j.epsl.2015.09.036.

Paulick, H., Bach, W., Godard, M., de Hoog, C.J., Suhr, G., Harvey, J., 2006. ODP Leg 209): implications for fluid /rock interaction in slow spreading environments. Chem. Geol. 234, 179–210. https://doi.org/10.1016/j.chemgeo.2006.04.011.

Peters, D., Bretscher, A., John, T., Scambelluri, M., Pettke, T., 2017. Fluid-mobile elements in serpentinites: Constraints on serpentinisation environments and element cycling in subduction zones. Chem. Geol. 466, 654–666. https://doi.org/10.1016/j.chemgeo.2017.07.017.

Piccardo, G.B., Zanetti, A., Müntener, O., 2007. Melt/peridotite interaction in the Southern Lanzo peridotite: field, textural and geochemical evidence. Lithos 94, 181–209. https://doi.org/10.1016/j.lithos.2006.07.002.

Poitrasson, F., Delpech, G., Gregoire, M., 2013. On the iron isotope heterogeneity of lithospheric mantle xenoliths : implications for mantle metasomatism, the origin of basalts and the iron isotope composition of the Earth. Contrib. Mineral. Petrol. 165, 1243–1258. https://doi.org/10.1007/s00410-013-0856-7.

Pokrovski, G.S., Sanchez-Valle, C., Guillot, S., Borisova, A.Y., Muñoz, M., Auzende, A.L., Proux, O., Roux, J., Hazemann, J.L., Testemale, D., 2022. Redox dynamics of subduction revealed by arsenic in serpentinite. Geochemical Perspect. Lett. 22, 36–41.

Polyakov, V.B., Mineev, S.D., 2000. The use of Mossbauer spectroscopy in stable isotope geochemistry. Geochim. Cosmochim. Acta 64, 849–865. https://doi.org/10.1016/S0016-7037(99)00329-4.

Rabin, S., Blanchard, M., Pinilla, C., Poitrasson, F., Grégoire, M., 2021. First-principles calculation of iron and silicon isotope fractionation between Fe-bearing minerals at magmatic temperatures: the importance of second atomic neighbors. Geochim. Cosmochim. Acta 304, 101–118.

Rapp, J.F., Klemme, S., Butler, I.B., Harley, S.L., 2010. Extremely high solubility of rutile in chloride and fluoride-bearing metamorphic fluids: an experimental investigation. Geology 38, 323–326.

Rojas-Kolomiets, E., Jensen, O., Bizimis, M., Yogodzinski, G., Ackerman, L., 2023. Serpentinite fluids and slab-melting in the Aleutian arc: evidence from molybdenum isotopes and boron systematics. Earth Planet. Sci. Lett. 603, 117970.

Salters, V.J.M., Stracke, A., 2004. Composition of the depleted mantle. Geochem. Geophys. Geosyst. 5 https://doi.org/10.1029/2003GC000597.

Scambelluri, M., Cannao, E., Gilio, M., 2019. The water and fluid-mobile element cycles during serpentinite subduction. A review. Eur. J. Mineral. 31, 405–428. https://doi.org/10.1127/ejm/2019/0031-2842.

Scambelluri, M., Pettke, T., Cannaò, E., 2015. Fluid-related inclusions in Alpine high-pressure peridotite reveal trace element recycling during subduction-zone dehydration of serpentinized mantle (Cima di Gagnone, Swiss Alps). Earth Planet. Sci. Lett. 429, 45–59. https://doi.org/10.1016/j.epsl.2015.07.060.

Scambelluri, M., Tonarini, S., 2012. Boron isotope evidence for shallow fluid transfer across subduction zones by serpentinized mantle. Geology 40, 907–910.

Schwartz, S., Allemand, P., Guillot, S., 2001. Numerical model of the effect of serpentinites on the exhumation of eclogitic rocks: insights from the Monviso ophiolitic massif (Western Alps). Tectonophysics 342, 193–206. https://doi.org/10.1016/S0040-1951(01)00162-7.

Schwartz, S., Guillot, S., Reynard, B., Lafay, R., Debret, B., Nicollet, C., Lanari, P., Auzende, A.L., 2013. Pressure-temperature estimates of the lizardite/antigorite transition in high pressure serpentinites. Lithos 178, 197–210. https://doi.org/10.1016/j.lithos.2012.11.023.

Scott, S.R., Sims, K.W.W., Frost, B.R., Kelemen, P.B., Evans, K.A., Swapp, S.M., 2017. On the hydration of olivine in ultramafic rocks: implications from Fe isotopes in serpentinites. Geochim. Cosmochim. Acta 215, 105–121. https://doi.org/10.1016/j.gca.2017.07.011.

Shaw, D.M., 1970. Trace element fractionation during anatexis. Geochim. Cosmochim. Acta 34, 287. –243.

Snow, J., Dick, J., 1995. Pervasive magnesium loss by marine weathering of peridotite. Geochim. Cosmochim. Acta 59, 4219–4235.

Sossi, P.A., Debret, B., 2021. The role of redox processes in determining the iron isotope compositions of minerals, melts and fluids. In: Moretti, R., Neuville, D.R. (Eds.), Magma Redox Geochemistry. John Wiley & Sons, Inc., pp. 303–330

Sossi, P.A., Halverson, G.P., Nebel, O., Eggins, S.M., 2015. Combined separation of Cu, Fe and Zn from rock matrices and improved analytical protocols for stable isotope determination. Geostand. Geoanalytical Res. 39, 129–149. https://doi.org/10.1111/j.1751-908X.2014.00298.x.

Sossi, P.A., Nebel, O., Foden, J., 2016. Iron isotope systematics in planetary reservoirs. Earth Planet. Sci. Lett. 1, 1–14. https://doi.org/10.1016/j.epsl.2016.07.032.

Sossi, P.A., Nebel, O., O'Neill, H.S.C., Moynier, F., 2018. Zinc isotope composition of the Earth and its behaviour during planetary accretion. Chem. Geol. 477, 73–84. https://doi.org/10.1016/j.chemgeo.2017.12.006.

Sossi, P.A., O'Neill, H.S.C., 2017. The effect of bonding environment on iron isotope fractionation between minerals at high temperature. Geochim. Cosmochim. Acta 196, 121–143. https://doi.org/10.1016/j.gca.2016.09.017.

Su, B.-X., Teng, F.-Z., Hu, Y., Shi, R.-D., Zhou, M.-F., Zhu, B., Liu, F., Gong, X.-H., Huang, Q.-S., Xiao, Y., 2015. Iron and magnesium isotope fractionation in oceanic lithosphere and sub-arc mantle: perspectives from ophiolites. Earth Planet. Sci. Lett. 430, 523–532.

Sun, S.S., McDonough, W.F., 1989. Chemical and isotopic systematics of oceanic basalts: implications for mantle composition and processes. Geol. Soc. Spec. Publ. 42, 313–345. https://doi.org/10.1144/GSL.SP.1989.042.01.19.

Tanis, E.A., Simon, A., Zhang, Y., Chow, P., Xiao, Y., Hanchar, J.M., Tschauner, O., Shen, G., 2016. Rutile solubility in NaF–NaCl–KCl-bearing aqueous fluids at 0.5–2.79 GPa and 250–650°C. Geochim. Cosmochim. Acta 177, 170–181.

Teng, F.Z., Dauphas, N., Huang, S., Marty, B., 2013. Iron isotopic systematics of oceanic basalts. Geochim. Cosmochim. Acta 107, 12–26. https://doi.org/10.1016/j.gca.2012.12.027.

Vieira Duarte, J.F., Piccoli, F., Pettke, T., Hermann, J., 2021. Textural and geochemical evidence for magnetite production upon antigorite breakdown during subduction. J. Petrol. 62, egab053. https://doi.org/10.1093/petrology/egab053.

Weyer, S., Ionov, D.A., 2007. Partial melting and melt percolation in the mantle: the message from Fe isotopes. Earth Planet. Sci. Lett. 259, 119–133. https://doi.org/10.1016/j.epsl.2007.04.033.

Williams, H.M., Bizimis, M., 2014. Iron isotope tracing of mantle heterogeneity within the source regions of oceanic basalts. Earth Planet. Sci. Lett. 404, 396–407. https://doi.org/10.1016/j.epsl.2014.07.033.

Williams, H.M., McCammon, C.A., Peslier, A.H., Halliday, A.N., Teutsch, N., Levasseur, S., Burg, J.P., 2004. Iron isotope fractionation and the oxygen fugacity of the mantle. Science (80-.) 304, 1656–1659. https://doi.org/10.1126/science.1095679.

Zhang, Y., Gazel, E., Gaetani, G.A., Klein, F., 2021. Serpentinite-derived slab fluids control the oxidation state of the subarc mantle. Sci. Adv. 7, 1–8. https://doi.org/10.1126/sciadv.abj2515.